Solid and Fluid Mechanics Simulations and their application to medical problems

Medsim Research Group. Universitat Rovira i Virgili.

MedSim Research Group

Gerard Fortuny[(1)]
Joan Herrero[(2)]
Josep M. López[(1)]
Dolors Puigjaner[(1)]

Physicians collaborators: Youcef Azeli (Sistema Emergències Mèdiques de Catalunya), Josep Garcia Bennet (Hospital de Bellvitge), Francesc Marimon (Hospital Sant Joan de Reus), Manuel López Cano (Hospital Vall d'Hebron)

(1) Departament d'Enginyeria Informàtica i Matemàtiques

(2) Departament d'Enginyeria Química

Main Objectives

To work in biomechanic problems.
To help answer questions arising from medical professional experience.

To use Open Source Software (OSS).

Inferior Vena Cava Filters (IVC)

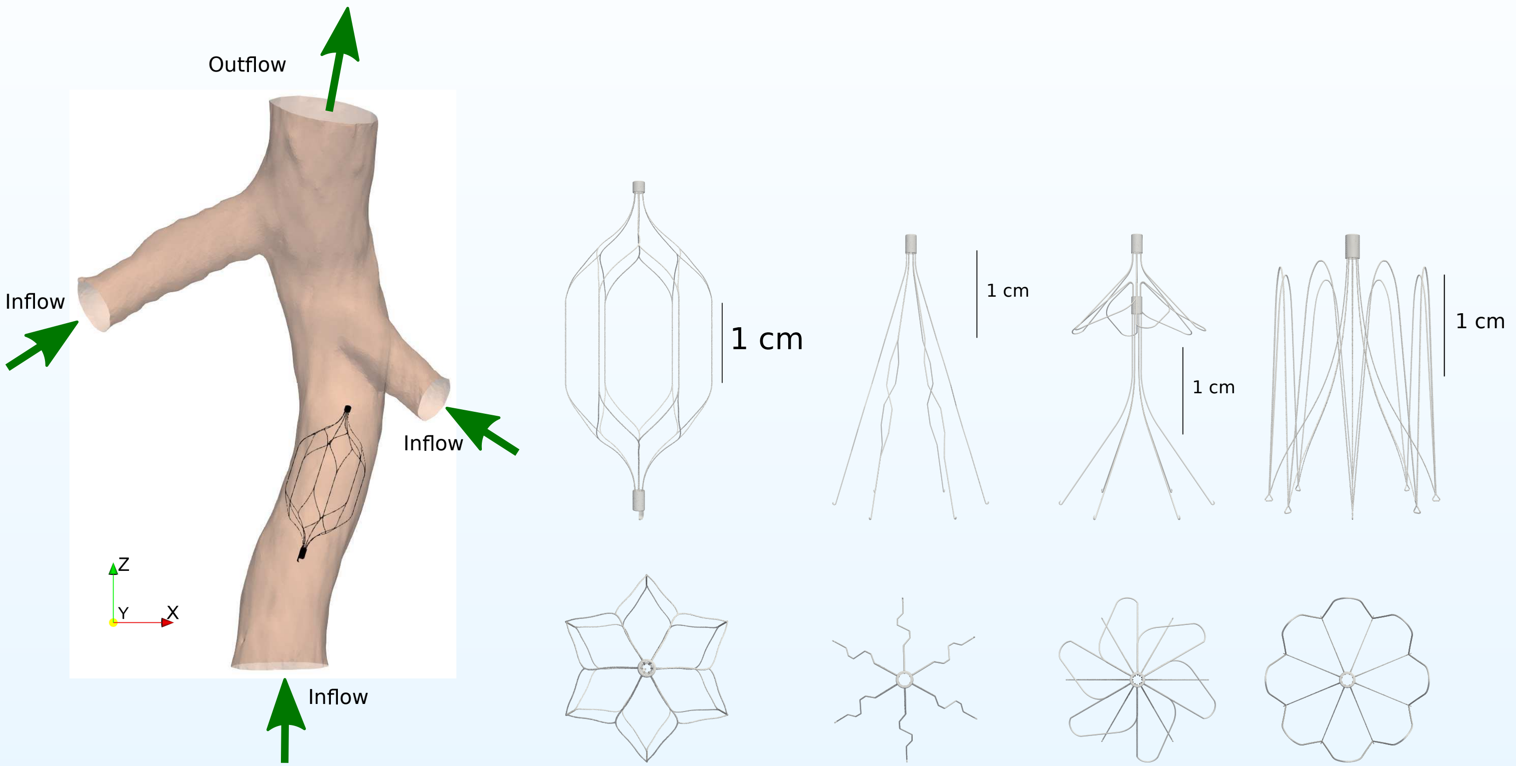

- IVC filters, which prevent blood clots migration and, are implanted to Deep Vein Thrombosis (DVT) patients.
- Several IVC filter models are available.
- How does the IVC filter model affect the hemodynamics of blood flow in the vein?

Clots in Inferior Vena Cava Filters

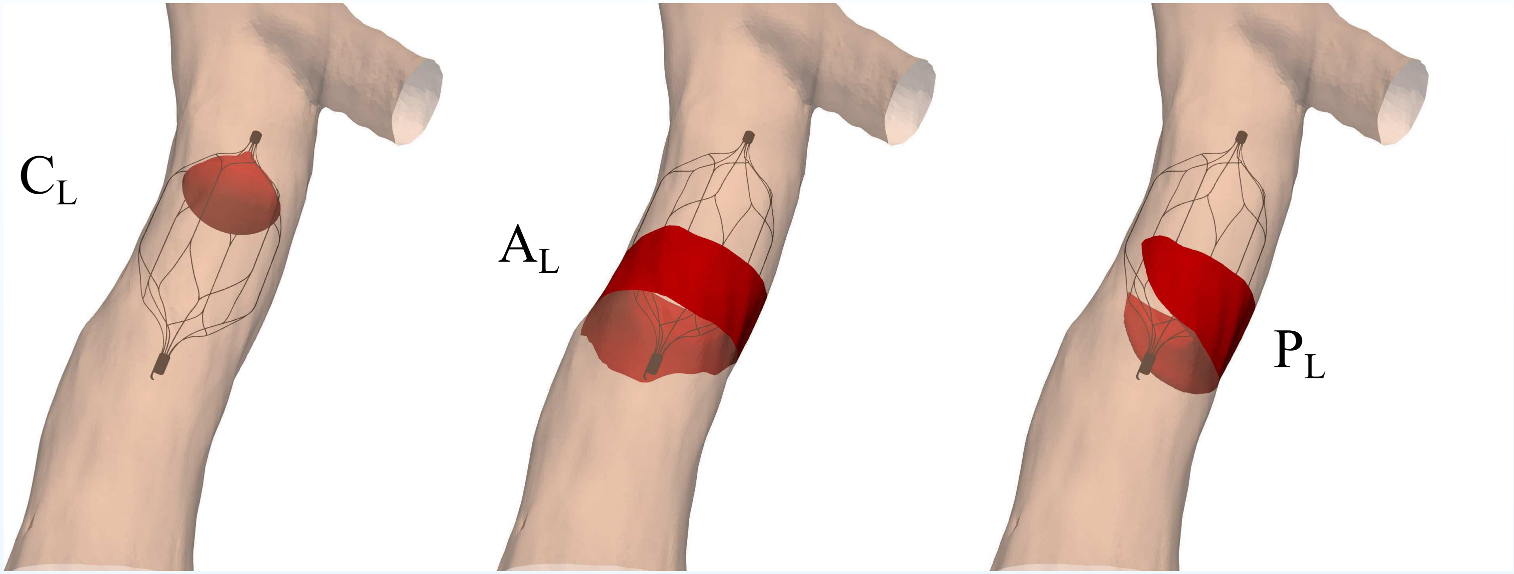

- IVC filters are designed to capture blood clots.
- Blood clots attached to the filters cause partial occlusion of the vein and alter the blood flow
- Cavograms show that clots tend to adapt to the shapes of the filter and vein wall.
- What are the effects on the blood flow of one or two clots attached to an OPTEASE IVC filter?

Cardiopulmonary Resuscitation (CPR)

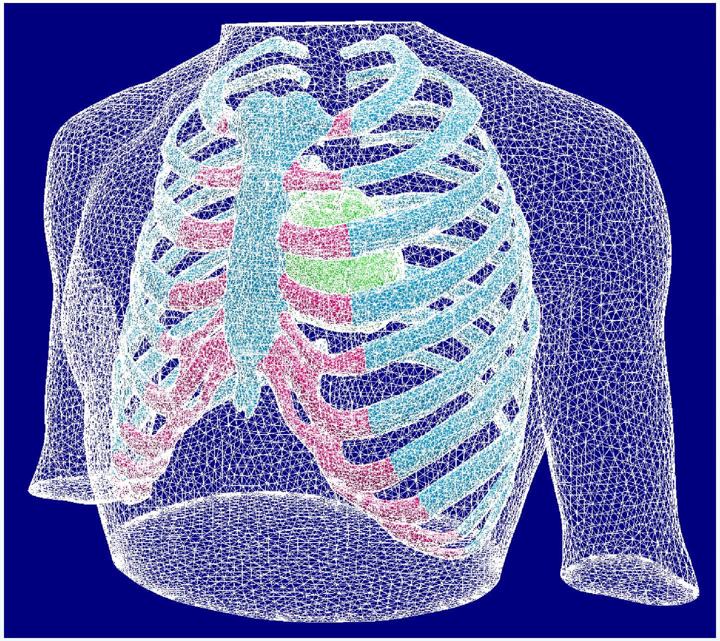

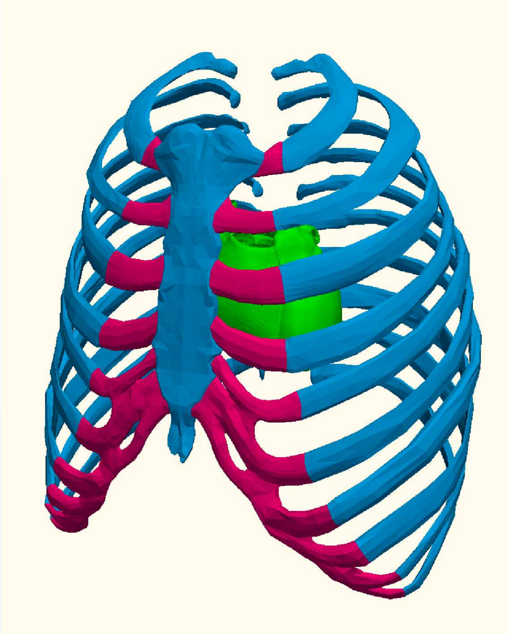

- CPR often implies fracture of one or more ribs.
- The optimal location of compression point and how the force exerted affects the thorax and the heart is unknown.
- Which is the effect of the compression location on the biomechanical response of the rib cage?

Dynamics of the Abdominal Wall

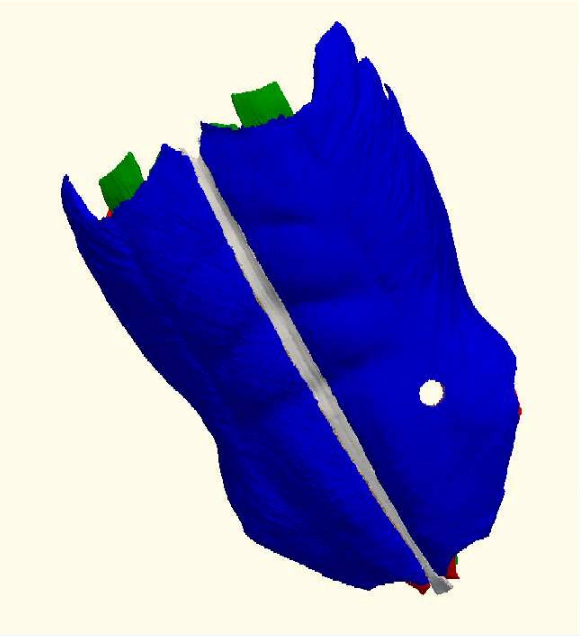

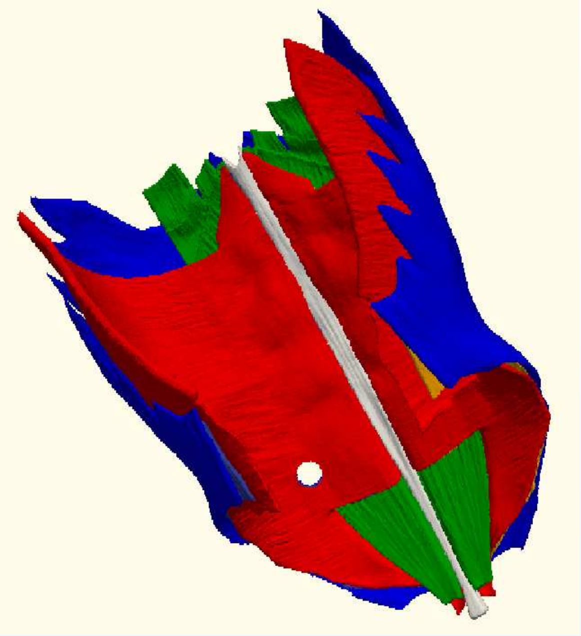

- Patients with an abdominal stoma are prone to suffer from parastomal hernias (PH)
- Enlargement of the stoma incision is generally considered a risk factor for PH
- Does the location of the stoma affects the abdominal wall mechanics and/or the enlargement of the stoma incision?

Dynamics in the Prostate region

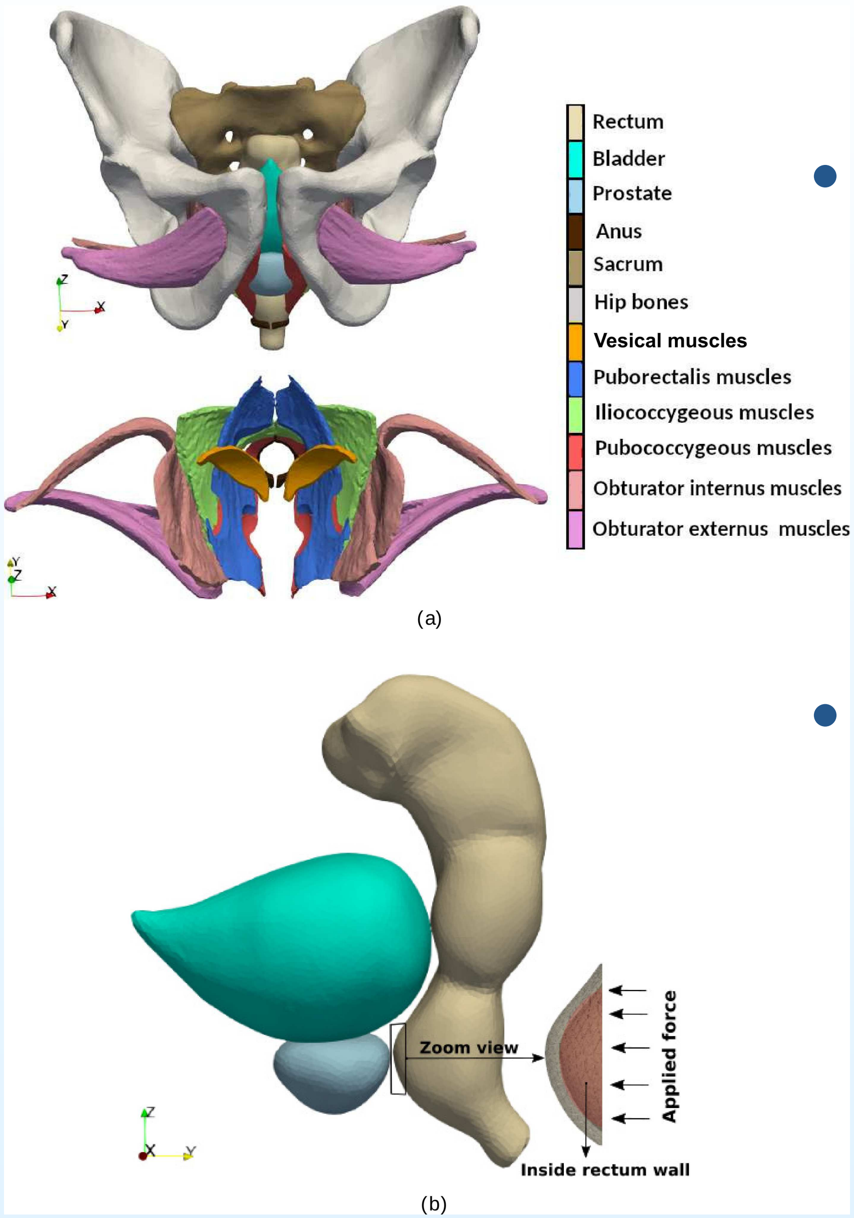

(a)

(b)

- Prostate neoplasms, visible in magnetic resonance images (MRI), are difficult to be located at the time of performing a transrectal ultrasound (TRUS) guided biopsy.
- Can we help to predict the location of prostate neoplasms during an MRI-TRUS fusion biopsy?

Geometry models: surface and 3D meshes

From in vivo computed tomography images to triangular surface meshes (Image Segmentation).
From triangular surface meshes to 3D tetrahedral meshes.

- 3D Slicer: a flexible modular platform for image analysis and visualization. It allows automatic image segmentation.
- SALOME: a platform for pre– and post–processing needs in numerical simulations. It offers a mesh generator/editor.
- CGAL: a C++ library with efficient and reliable geometric algorithms. It offers algorithms related to triangulations and surface and volume mesh generation.
- Gmsh: a finite–element mesh generator
- Self–made code developed in the MedSim Group.

Numerical simulations

- OpenFOAM is an Open Source software for Computational Fluid Dynamics (CFD).
- Code Aster is an Open Source software package for Civil and Structural Engineering (Solid Mechanics).
- MFront is a code generation tool dedicated to the implementation of arbitrary complex mechanical behaviors (material constitutive equations) (Solid Mechanics).

Other Software

ParaView — Visualization

GNU, GCC — Operating System and Compiler

Self–made code developed in the MedSim Group.

Inferior Vena Cava Filters Problem

Motivation

- Pulmonary embolism (PE) occurs when a blood clot becomes lodged in the pulmonary vascular system and obstruct blood flow.
- Most often PE is a consequence of deep venous thrombosis (DVT).
- Venous thromboembolism (DVT and/or PE) has an incidence of 1.4 to 2.2 per 1000 persons–year among US citizens aged over 45, and mortality rate is approximately 25% in the first 30 days.
- DVT patients are often treated with anticoagulant drugs and/or placement of a IVC filter.
- Partial occlusion of the vein due to the presence of clots leads to the appearance of regions with flow recirculation or even turbulent flow.
- Recirculating flow regions would be prone to become areas of thrombogenesis.

Objectives

- To build a realistic numerical model of a portion of vena cava and filters
- To study the effects of vena cava filters on blood flow by means of a computer simulation
- To make a hemodynamic comparison of different filter models
- To build realistic numerical models of clots with shapes adapted to the geometries of the filter and/or the vein wall.
- To assess the effects on the blood flow (stagnation, recirculation zones, instabilities, turbulence) of one or two clots attached to an OPTEASE IVC filter.

Geometry model

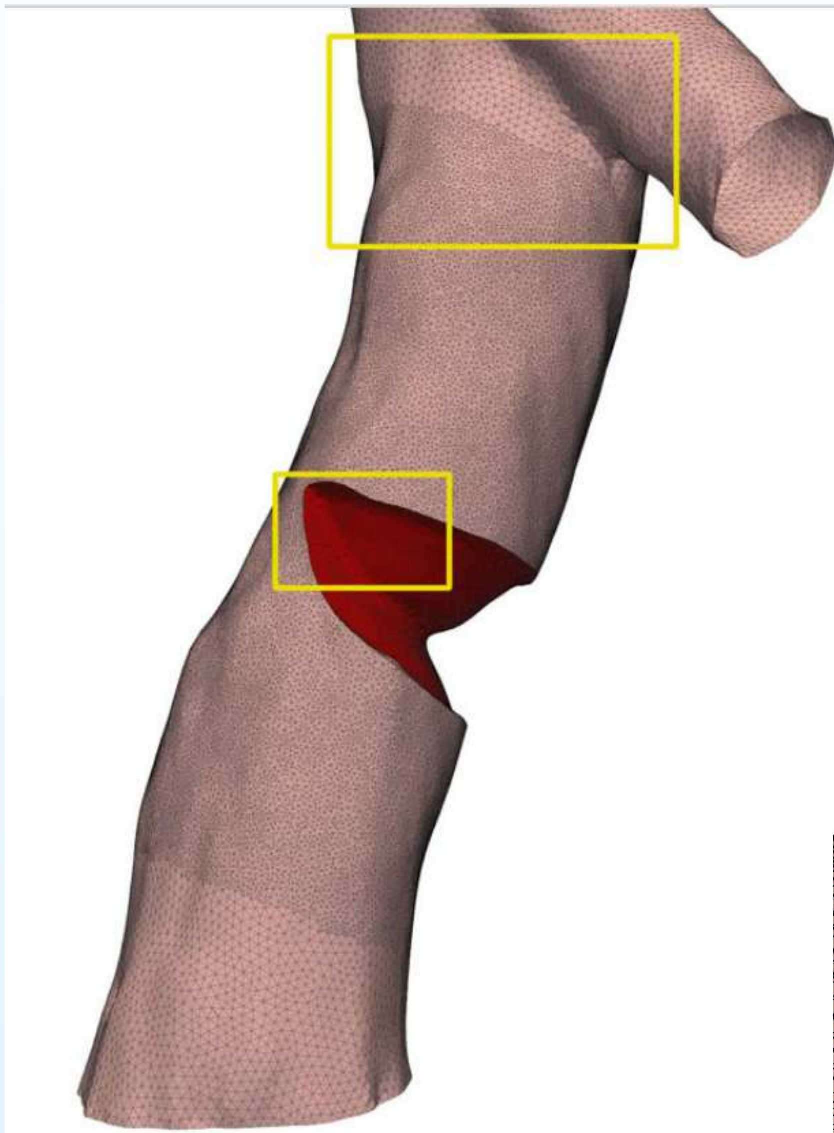

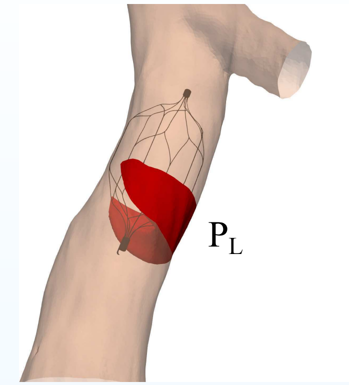

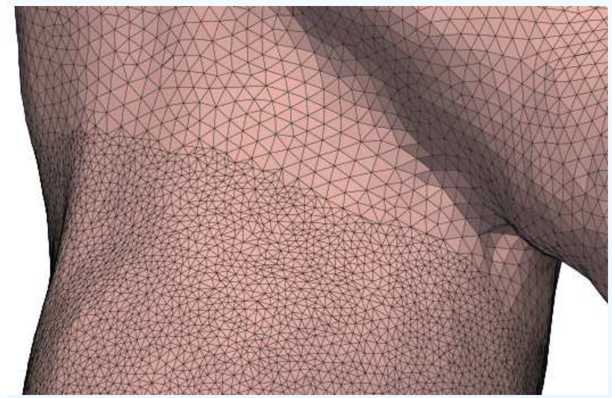

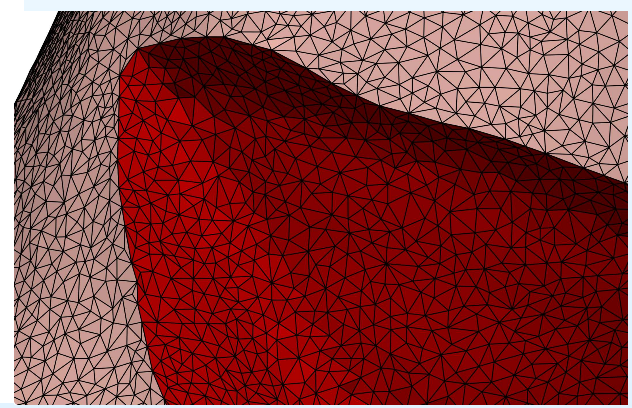

Computational meshes

Triangular surface meshes

- vein without filter: 68,432 triangles
- vein with filters: refined up to 72,098 triangles
- vein with filters and clots: refined up to 104,973 triangles
- filters: between 55,032 and 130,468 triangles

3D meshes

- between 301,389 and 12,040,516 tetrahedra

Clot model generation

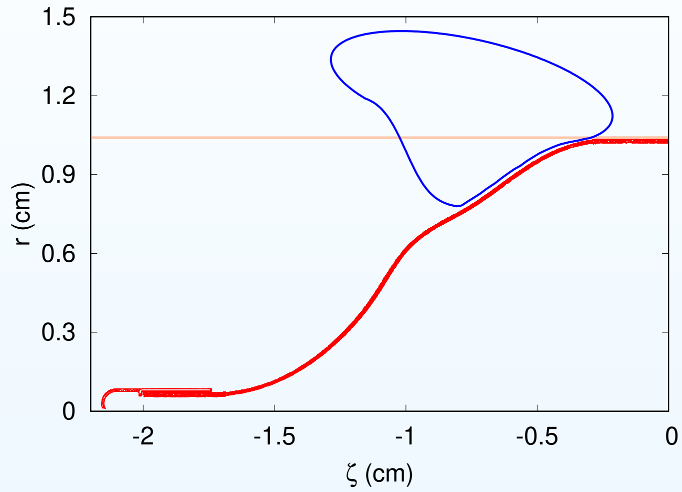

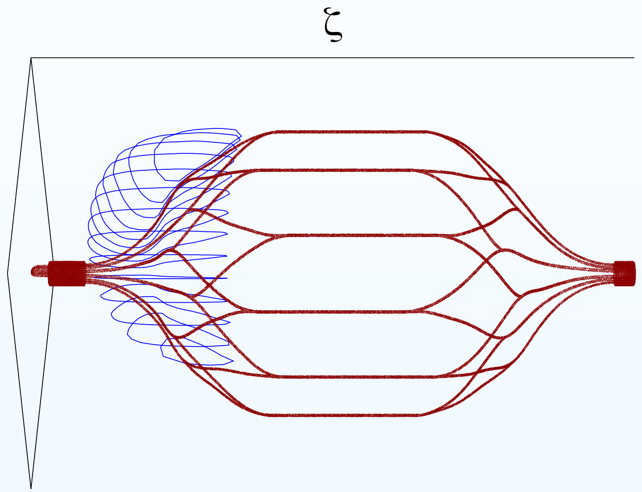

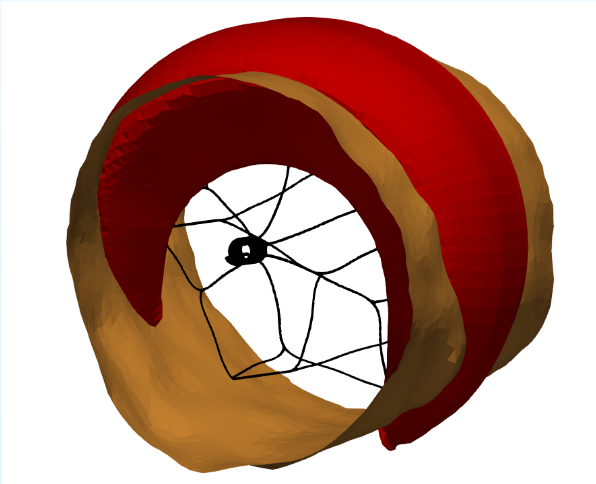

Conservation equations for incompressible fluids

$$\frac{\partial U}{\partial t} + (U \cdot \nabla) U = -\frac{1}{\rho}\nabla p + \left\{ \nabla \cdot \left[\left(\frac{\mu + \mu_T}{\rho} \right) \nabla \right] \right\} U$$

$$\nabla \cdot U = 0$$

$U = (u_x, u_y, u_z)$ is the velocity vector
p is the pressure
ρ and μ are the fluid density and viscosity
$\mu_T/\rho = \nu_T$ is the turbulent kinematic viscosity

- Non–Newtonian Bird–Carreau viscosity model
- Walters and Cokljat $k_L - k_T - \omega$ closure model for the turbulent viscosity, ν_T
- Different blood flow rates, from rest (20 cm^3/s) to exercise (80 cm^3/s)

Wall shear stress on vein in the absence of clots

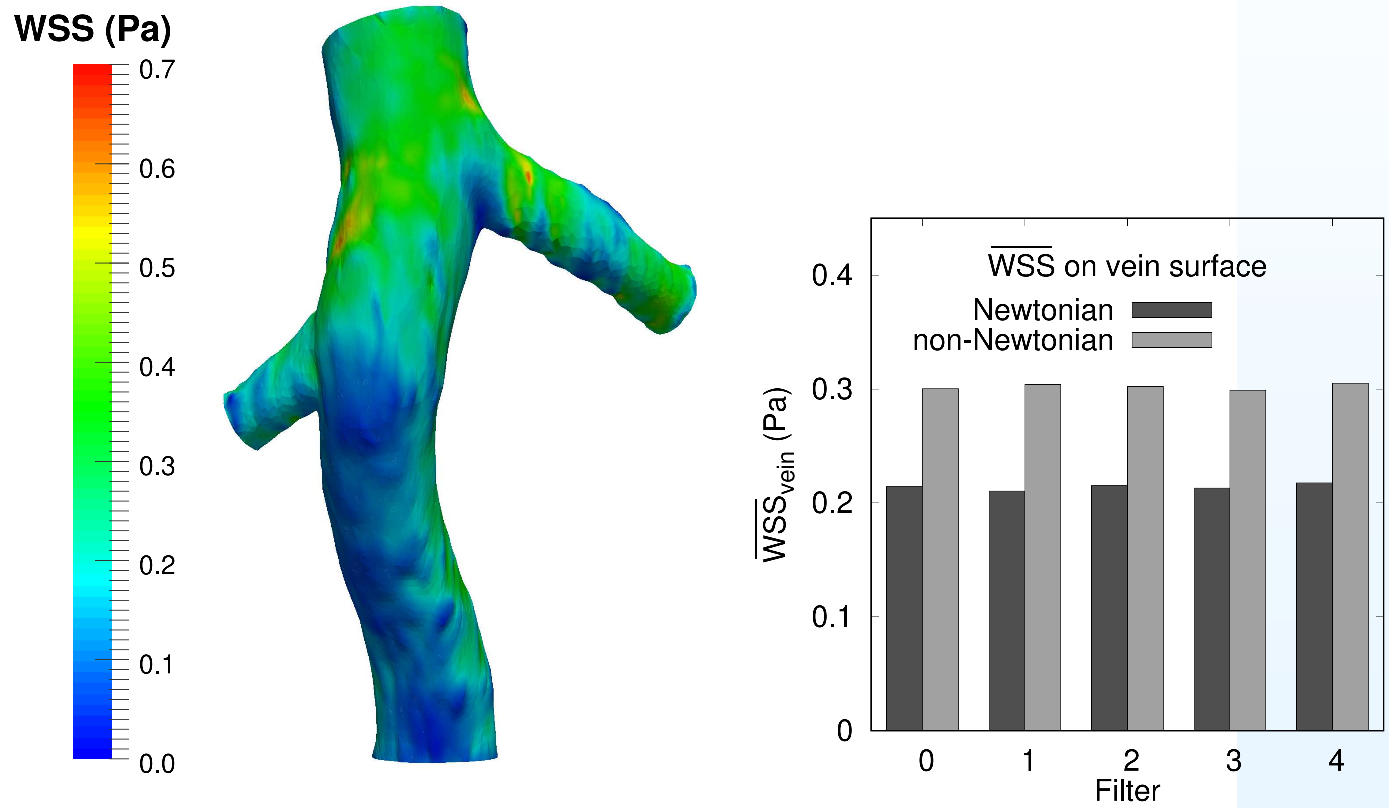

- WSS distribution largely affected by geometry in all cases
- Filters cause little variation of WSS averages on vein

Force/Velocity on filters in the absence of clots

Forces

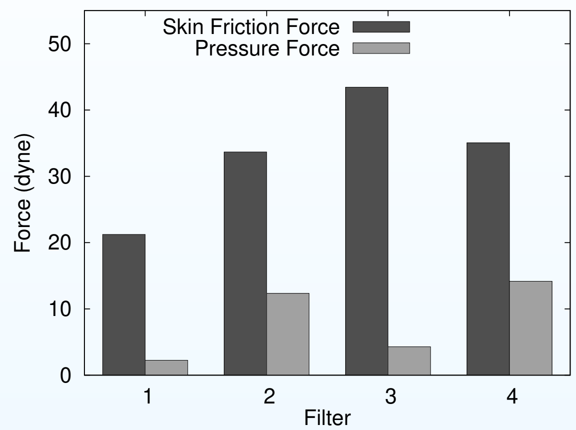

Rest

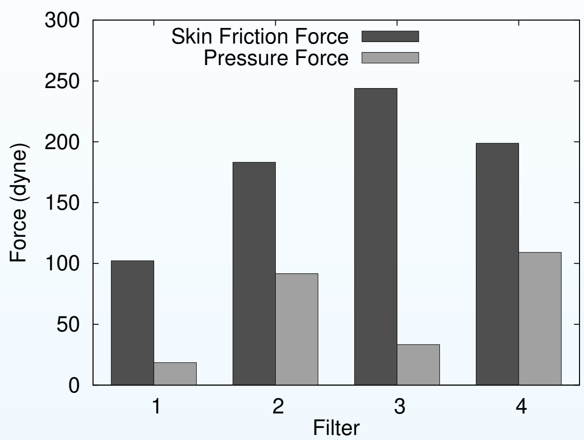

Exercise

Blood velocity

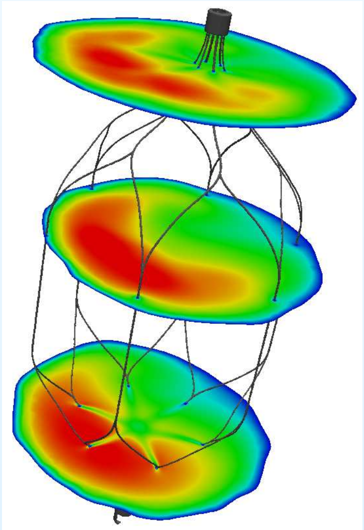

Flow recirculation in the presence of clots

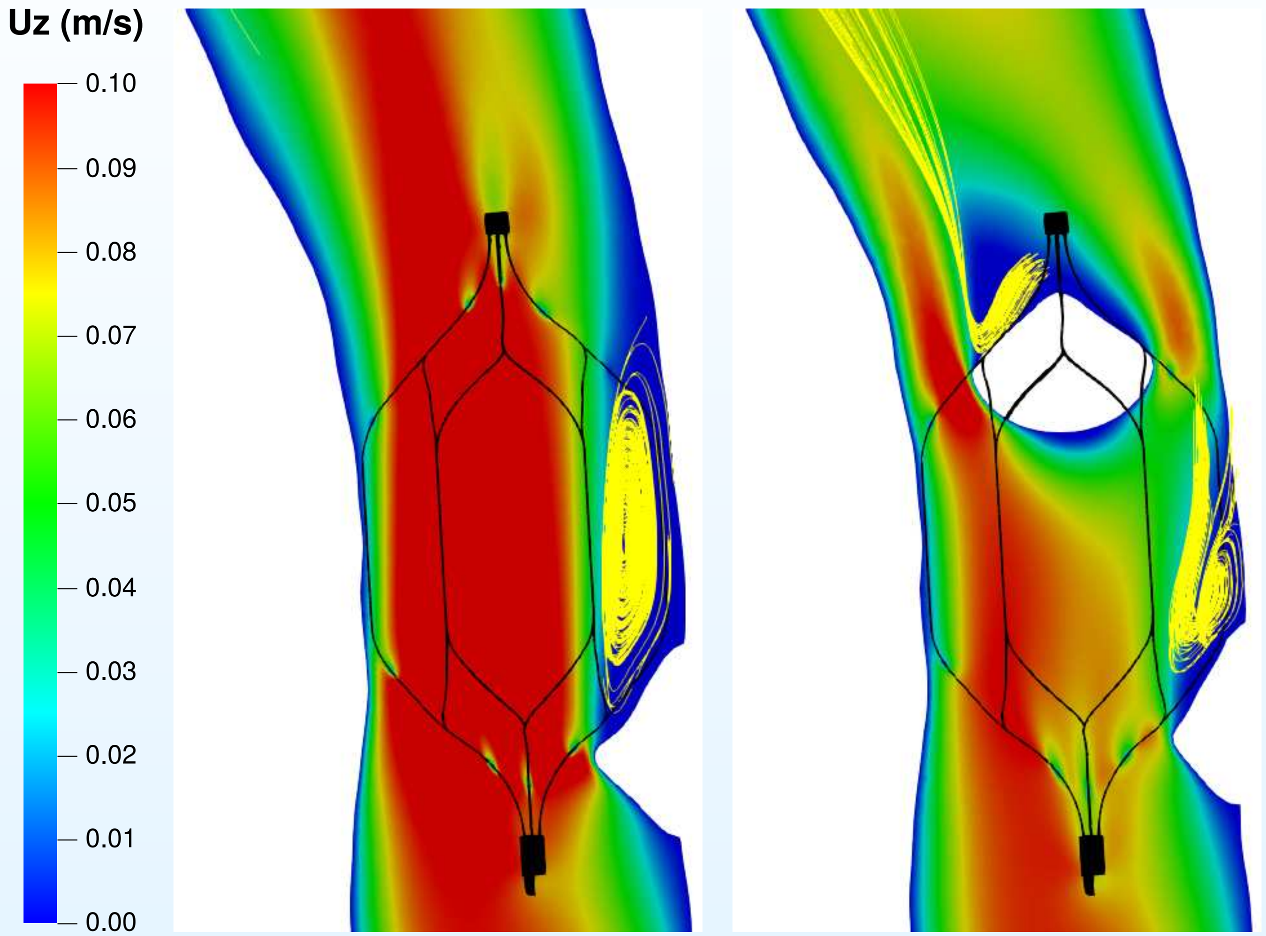

Time periodic solutions

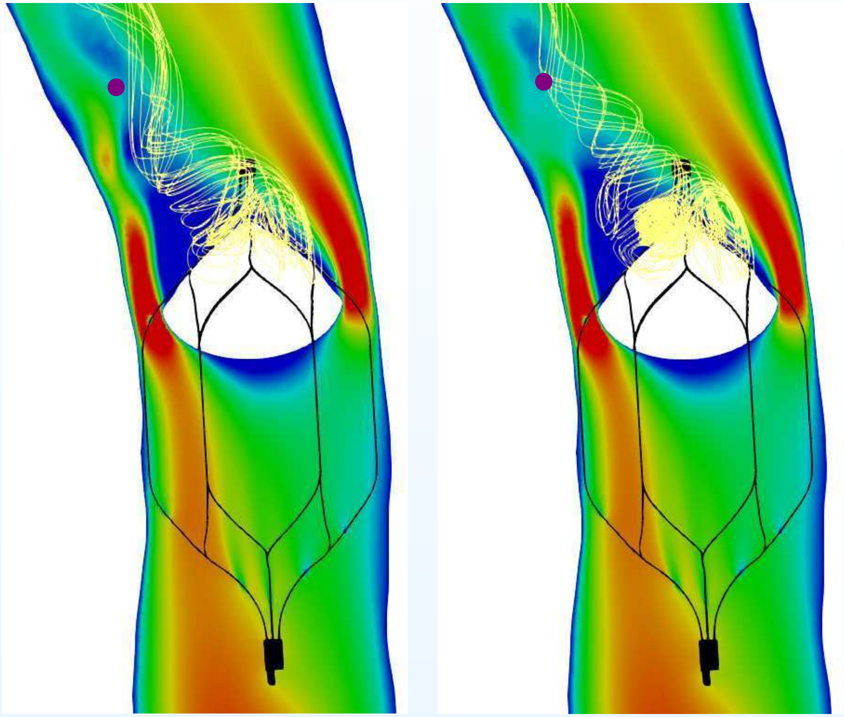

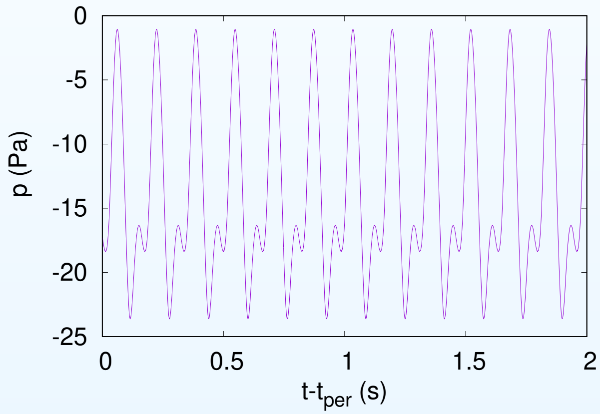

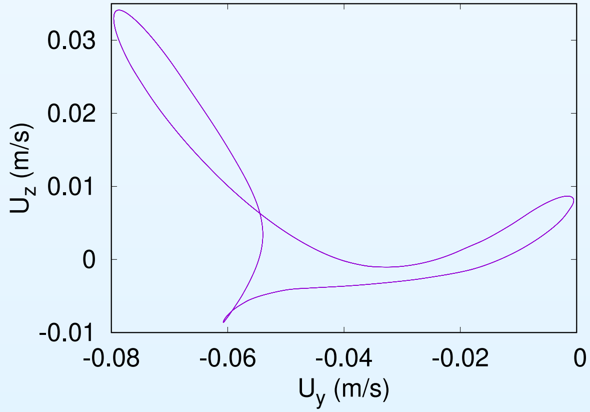

Time evolution

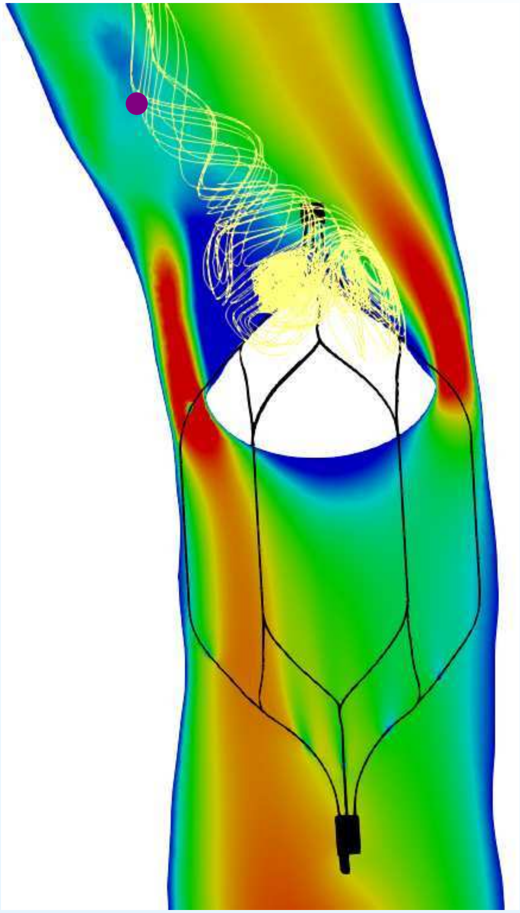

Conclusions

- The presence of a filter has little effect on the overall values of blood flow velocity or wall shear stress
- Under exercise conditions the magnitude of the forces exerted on the filters and on the clots by the blood flow are, respectively, not negligible and considerable. These forces must be counterbalanced by forces exerted by the hooks/struts on the vein wall
- High levels of flow stagnation occur in rest conditions in the wake of clots placed upstream from the filter.
- One downstream placed big clot induce higher flow instabilities than two small clots placed in tandem.
- These results may be accounted for medical complications related to filters, such as tissue perforation, filter tilting, filter migration or thrombogenesis

Abdominal Wall

Muscular tissue

- Muscular tissue is often assumed to have a linear elastic behavior
- Experiments indicate that muscular tissue has indeed a highly hyperelastic nonlinear and anisotropic behavior with a ground isotropic contribution reinforced by one (or two) families of fibers (transversely isotropic hyperelastic behavior).

A constitutive equation for the transversely isotropic hyperelastic model can be written as:

$$\boxed{W_f = W_{fm} + W_{ff}}$$

where W denotes the strain energy function or Helmholtz free–energy function.

A simple example

$$W_{fm} = \frac{\mu_f}{2}\left(\tilde{I}_1 - 3\right) + \frac{k_{fv}}{2}\left(J^2 - 1 - 2\ln J\right)$$

$$W_{ff} = \frac{\alpha_{f1}}{2\alpha_{f2}}\left[\exp\left(\alpha_{f2}\left(\tilde{I}_4 - 1\right)^2\right) - 1\right]$$

$\tilde{I}_j$ invariants of C

$C = F^T F$ right Cauchy–Green symmetric tensor

F deformation gradient

$J = \det F$

Tensors

We need the Piola-Kirchhoff stress tensor

$$S = 2\frac{\partial W_{fm}}{\partial \tilde{C}} + 2\frac{\partial W_{ff}}{\partial \tilde{C}} = S^m + S^f$$

and the elasticity tensor:

$$\frac{\partial S}{\partial \tilde{C}} = \frac{\partial S^m}{\partial \tilde{C}} + \frac{\partial S^f}{\partial \tilde{C}}$$

MFront: Variables

We generate a text file with specific code

```
@Parser DefaultFiniteStrainParser; // this behaviour does not require an integration algorithm
@Behaviour pachera;
@Date 10/01/2018;

@Parameter mu_f    = 2.6e5;
@Parameter k_fv    = 2e9;
@Parameter alfa_f1 = 4.5e5;
@Parameter alfa_f2 = 45.68;

/* local variable to store the consistent tangent operator */
@LocalVariable StiffnessTensor dS_dC;

/* equations to solve */

@Integrator{
const Stensor id = Stensor::Id();                    // The identity tensor is stored in the id variable for a shorter and cleaner code
const real J  = det(F1);                             // Jacobian deformation (determinant of the deformation gradient at the end of the time ste
const Stensor C  = computeRightCauchyGreenTensor(F1);   // Right Cauchy tensor

/* invariants */
const real I1 = trace(C);                       // First invariant is the trace of C
const Stensor aux_C2 = square(C);                       // Needed for second invariant, I2 [square(C)=C^2]
const real I2 = (I1*I1-trace(aux_C2))/2;        // Second invariant
const real I3 = J*J;                            // Third invariant [I3=det(C)=det(F*F)=det(F)*det(F)=J*J]

/* volume-preserving part (Cbar) */
const real aux_J23 = cbrt(J*J);                                 // Cubic root of the square of J
const Stensor Cbar = (1/aux_J23)*C;                             // Modified Right Cauchy tensor

/* invariants with bars */
const real I1bar = trace(Cbar);                                 // First invariant of Cbar
const Stensor aux_C2bar = square(Cbar);
const real I2bar = (I1bar*I1bar-trace(aux_C2bar))/2;            // Second invariant of Cbar
tvector<3u,real> aux_n0;                        // Initial orientation (unit vector)
aux_n0(0)=0;
aux_n0(1)=0;
aux_n0(2)=1;
const Stensor aux_n0_n0 = Stensor::buildFromVectorDiadicProduct(aux_n0);
const real I4bar = Cbar|aux_n0_n0;
```

MFront: Stress tensor

We can compute the Piola-Kirchhoff stress tensor operating with 2D tensors

```
/* derivative of the invariants with bars */
const Stensor dI1bar_dCbar = id;                                // Derivative of I1bar
const Stensor dI2bar_dCbar = I1bar*id-Cbar;                     // Derivative of I2bar
const Stensor dI3bar_dCbar = aux_C2bar-I1bar*Cbar-I2bar*id;     // Derivative of I3bar (In TFEL 3.1, one may use the computeDeterminantDerivative)
const Stensor dI4bar_dCbar = aux_n0_n0;                         // Derivative of I4bar

// Wf=Wfm+Wff (energy function)

//SECOND PIOLA-KIRCHHOFF STRES (PK2)

// GROUND MATRIX
// Wfm=(mu_f/2)*(I1bar-3)+(k_fv/2)*(J^2-1-2lnJ)
// dWfm_dCbar   =dWfm_dI1bar*dI1bar_dCbar+dWfm_dI3bar*dI3bar_dCbar
//              =dWfm_dI1bar*dI1bar_dCbar+(1/2J)*dWfm_dJ*dI3bar_dCbar   [dI3bar=2J*dJ]
// Sfm = 2*dWfm_dCbar

const real aux_J2 = J*J;
const StressStensor Sfm = mu_f*dI1bar_dCbar+k_fv*(1-(1/aux_J2))*dI3bar_dCbar;

// COLLAGEN FIBERS
// Wff=[alfa_f1/(2*alfa_f2)]*[exp(alfa_f2*(I4bar-1)^2)-1]
// dWff_dCbar=dWff_dI4bar*dI4bar_dCbar
// Sff=2*dWff_dCbar

const real aux_I4bar_1 = I4bar-1;
const StressStensor Sff = 2*alfa_f1*aux_I4bar_1*exp(alfa_f2*aux_I4bar_1*aux_I4bar_1)*dI4bar_dCbar;

// CAUCHY STRESS
sig = convertSecondPiolaKirchhoffStressToCauchyStress(Sfm+Sff,F1);      // Converts the PK2 stress to the Cauchy Stress using the deformation gradient
```

MFront: Elasticity tensor

We can compute the elasticity tensor operating with 4D tensors

```
// CONSISTENT TANGENT OPERATOR

        if(computeTangentOperator_){

        /* second derivative of the invariants with bars */
        const Stensor4 d2I3bar_dCbar2=Stensor4::dsquare(Cbar)-(Cbar^id)-I1bar*Stensor4::Id()+(id^dI2bar_dCbar);
        //The computeDeterminantSecondDerivative is not available. It can be replaced by the following code: Stensor4::dsquare(C)-(C^id)-I1*Stensor4::Id()+(id^dI2_dC)


        // GROUND MATRIX
        const Stensor4 dSm_dCbar=k_fv*(1-(1/aux_J2))*d2I3bar_dCbar2;

        // COLLAGEN FIBERS
        const real aux_1=1+2*alfa_f2*aux_I4bar_1*aux_I4bar_1;
        const Stensor4 aux_2=aux_n0_n0^aux_n0_n0;
        const real aux_3=exp(alfa_f2*aux_I4bar_1*aux_I4bar_1);
        const Stensor4 dSf_dCbar=2*alfa_f1*aux_3*aux_1*aux_2;

        dS_dC = dSm_dCbar+dSf_dCbar;
        }
}

@TangentOperator<DS_DC>{
  Dt = dS_dC;
}
```

Rectus Abdominis muscle

$$W_{fm} = C_1\left(\tilde{I}_1 - 3\right) + C_2\left(\tilde{I}_1 - 3\right)^2 + \frac{k}{2}\left(J^2 - 1 - 2\ln J\right)$$

$$W_{ff} = C_3\left(\tilde{I}_4 - 1\right)^2 + C_4\left(\tilde{I}_4 - 1\right)^4$$

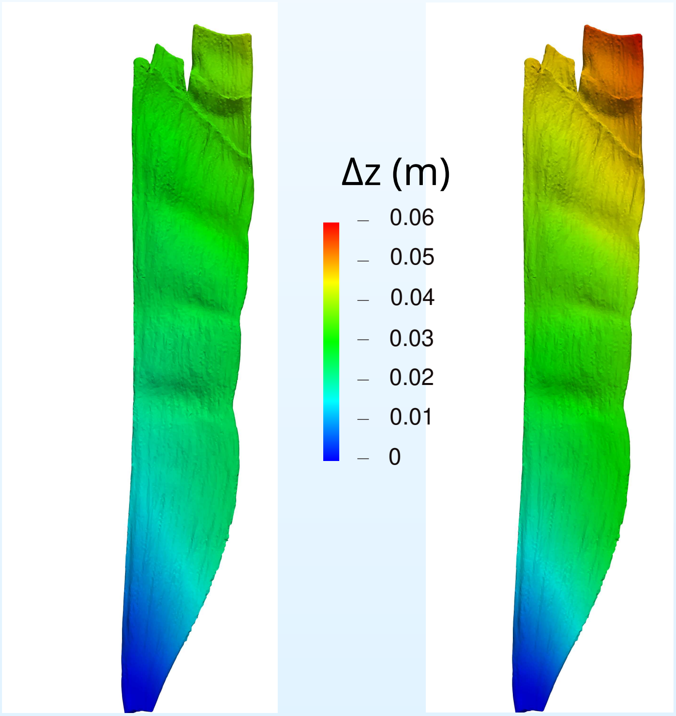

Abdominal wall geometry

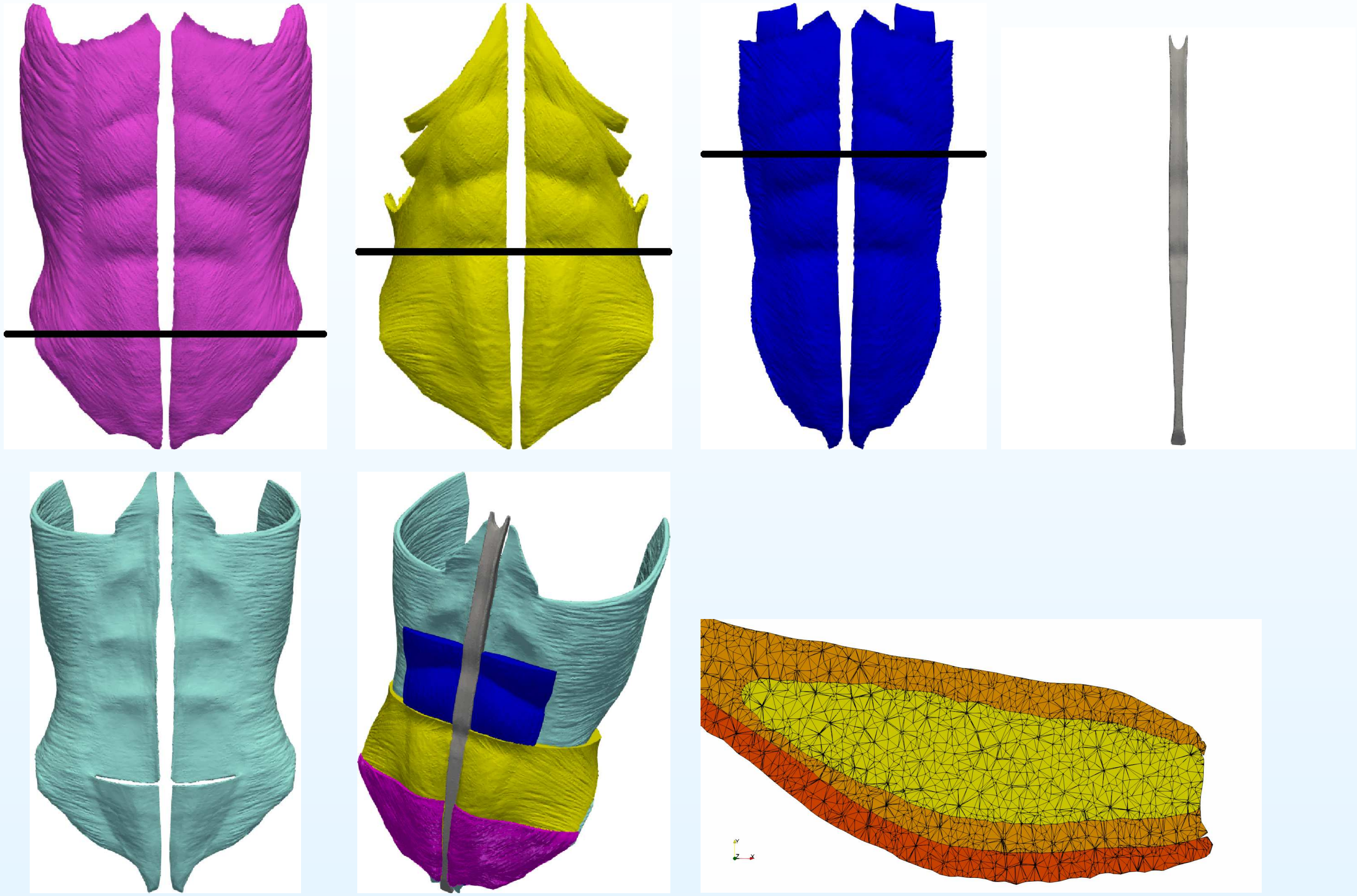

Deformation of abdominal wall with stomas

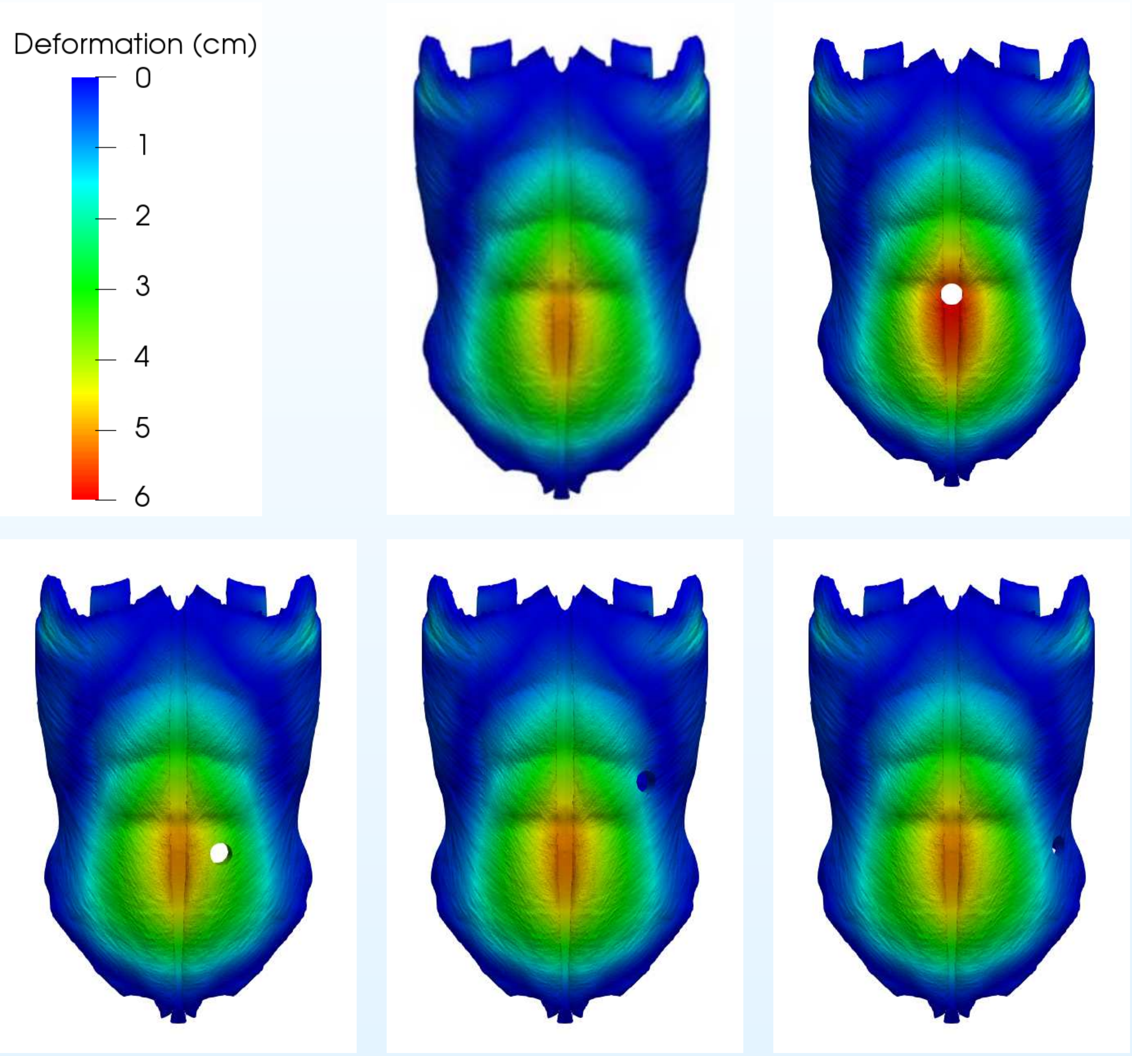

Deformation of stomas

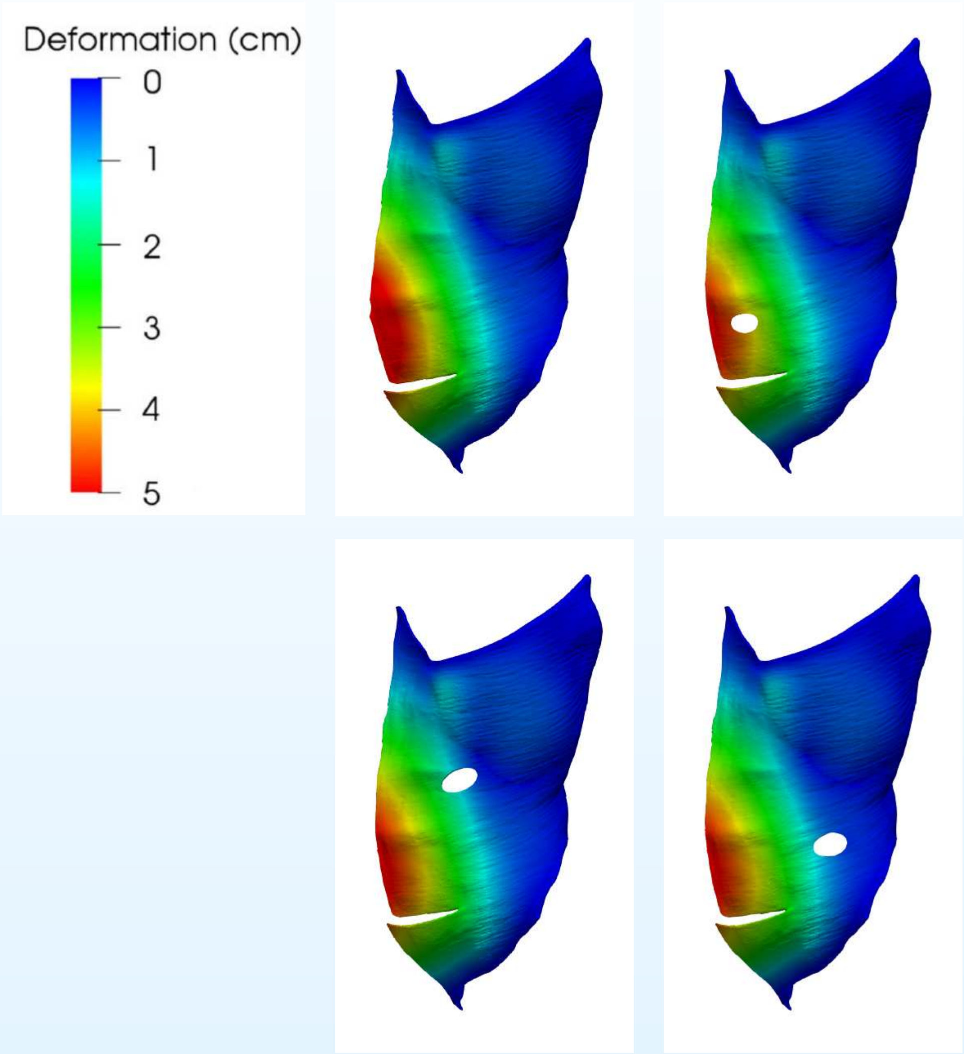

Conclusions

- The amount of deformation of the abdominal wall and the stress levels that it supports show a very weak dependence on stoma location, except for the case with a stoma located on the linea alba.
- Stoma perimeter and area respectively increase by as much as 44% and 85% .
- Stomas placed lateral to the Rectus abdominis muscle experience higher enlargements
- Creation of stomas located either on the linea alba or lateral to the Rectus Abdominis ought to be avoided.

CPR Results

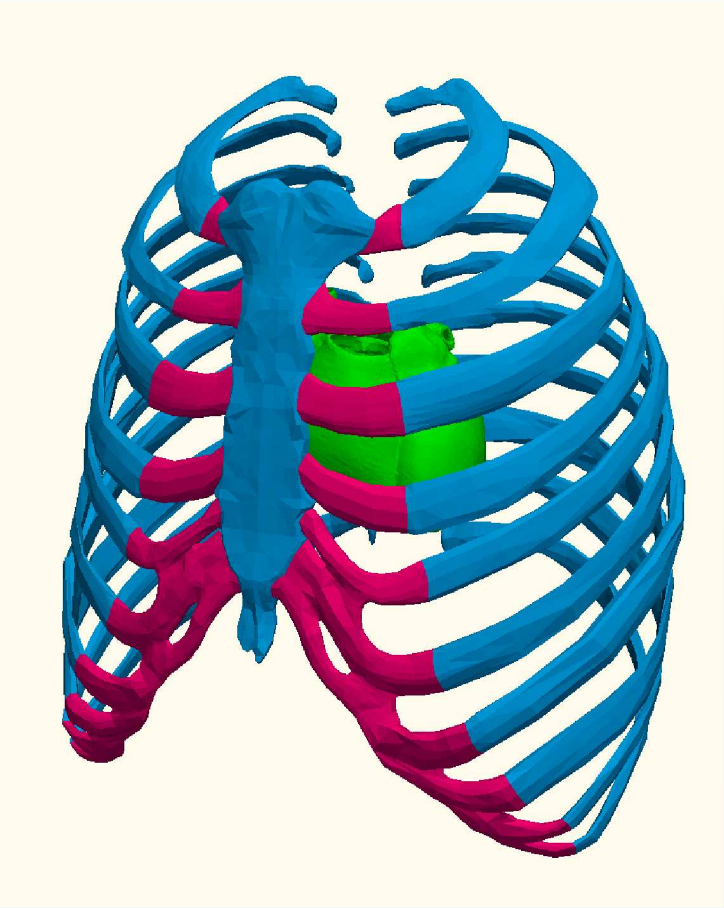

Viscoelastic Brick

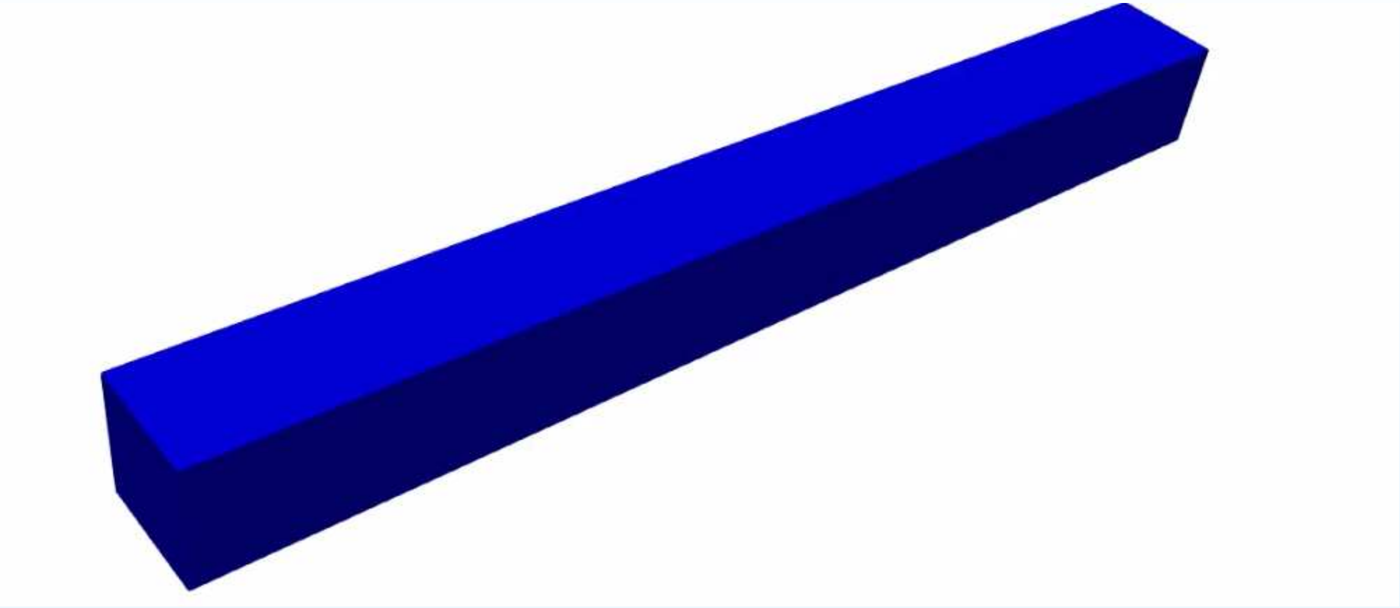

Conclusion

Computer simulations can be a valuable tool to study medical problems and to provide information that can help doctors to take decisions.

Publications

Tuset, L., Fortuny, G., Herrero, J., Puigjaner, D. and López, J.M. "Implementation of a new constitutive model for abdominal muscles", *Computer Methods and Programs in Biomedicine*, **179** 104988 (2019)

López, J.M., Fortuny, G., Puigjaner, D., Herrero, J., and Marimon, F. "Hemodynamic effects of blood clots trapped by an inferior vena cava filter", *Int J Numer Meth Biomed Engng.*, **36** e3343 (2020)

Tuset, L., López–Cano, M., Fortuny, G., López, J.M., Herrero, J. and Puigjaner, D. "Virtual simulation of the biomechanics of the abdominal wall with different stoma locations", *Scientific Reports*, **12** 3545 (2022)

Suazo, M., Herrero, J., Fortuny, G., Puigjaner, D. and López, J.M. "Biomechanical response of human rib cage to cardiopulmonary resuscitation maneuvers: Effects of the compression location", *Int J Numer Meth Biomed Engng.*, e3585 (2022)

Qasim, M., Puigjaner, D., Herrero, J., López, J.M., Olivé, C., Fortuny, G. and Garcia–Bennett, J. "Biomechanical modelling of the pelvic system: improving the accuracy of the location of neoplasms in MRI-TRUS fusion prostate biopsy", *BMC Cancer*,**22** 338 (2022)